JOC*Article*

Structural Studies on Cycloadducts of Furan, 2-Methoxyfuran, and 5-Trimethylsilylcyclopentadiene with Maleic Anhydride and *N*-Methylmaleimide

Yit Wooi Goh, Brett R. Pool, and Jonathan M. White*

School of Chemistry and Bio-21 Institute, The University of Melbourne, Parkville Vic 3010, Australia

whitejm@unimelb.edu.au

Received August 24, 2007

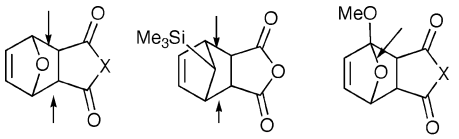

13, **15**, **16** **9** **21** X = O **22** X = NMe

The early stages of the retro-Diels−Alder reaction are clearly apparent in the structures of the cycloadducts formed between furan or 5-trimethylsilylcyclopentadiene with maleic anhydride and *N*-methylmaleimide. The degree of lengthening of the C−C bonds that break in this reaction is clearly related to the known reactivity of these cycloadducts toward this reaction. In the structures of the cycloadducts **21** and **22** derived from 2-methoxyfuran, the early stages of an alternative fragmentation reaction are apparent, consistent with the reactivity of these compounds in solution.

Introduction

We have reported the structures of Diels−Alder cycloadducts formed between cyclopentadiene and cyclohexadiene derivatives with a variety of dienophiles including maleic anhydride, *N*-methylmaleimide, and benzoquinone.[1−4] These compounds were characterized using X-ray crystallography and by the determination of their $^{13}C-^{13}C$ 1-bond coupling constants in solution. In these structures the C−C bonds (indicated **a** and **b**), which are broken in the retro-Diels−Alder (rDA) reaction, were found to be lengthened compared to similar C−C bonds in model substrates, which do not undergo this pericyclic fragmentation process.

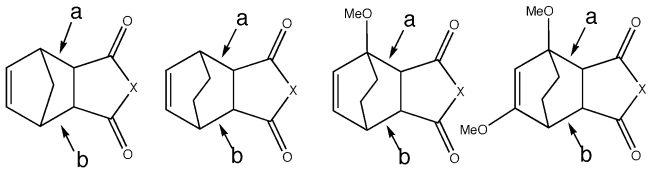

1): X = O
2): X = NMe
3): X = CH=CH

4): X = O
5): X = NMe
6): X = CH=CH

7): X = CH=CH

8): X = O

These are examples of the structure correlation principle,[5] which states that structural changes which occur along a reaction coordinate manifest in the ground state structure as deviations of bond distances from their normal values along the reaction coordinate. Compounds **1**−**6** which have been computed to undergo synchronous rDA reactions show similar degrees of lengthening for both bonds **a** and **b** in the ground state,[2] and in addition the degree of lengthening was found to correlate qualitatively with the known rDA reactivity of these cycloadducts.

In adduct **7**, which undergoes an asynchronous rDA reaction, bond **a** is lengthened to a significantly greater degree than bond **b**, which reflects the differences in these distances in the calculated transition state for the reaction. The crystal structure of the dioxygenated adduct **8** shows significant lengthening of bond **a** while bond **b** was "normal", leading to the prediction of a stepwise retro-Diels−Alder reaction for this derivative.[4]

The aim of this work was to obtain structural data on a range of Diels−Alder cycloadducts spanning a wider range of reactivities toward the rDA reaction, to further our understanding of the relationship between the degree of C−C bond lengthening in these adducts and their rDA reactivity. To this end we chose two classes of compound for this study, the trimethylsilyl-

(1) Pool, B. R.; White, J. M. *Org. Lett.* **2000**, *2*, 350.

(2) Birney, D.; Lim, T. K.; Peng, J.; Pool, B. R.; White, J. M. *J. Am. Chem. Soc.* **2002**, *124*, 5091.

(3) Goh, Y.G.; Danczak, S. M.; Lim, T. K.; White, J. M. *J. Org. Chem.* **2007**, 72, 2929.

(4) Goh, Y. W.; White, J. M. *Org. Biomol. Chem.* **2007**, 5, 2354.

(5) Burgi, H. B.; Dunitz, J. D. *Acc. Chem. Res.* **1983**, *16*, 153.

10.1021/jo7018575 CCC: $40.75
Published on Web 12/11/2007

TABLE 1. Selected Bond Distances for 1 and 9

cycloadduct	bond **a**	bond **b**	average (**a** and **b**)
1	1.569(2)	1.570(2)	1.570
9	1.579(2)	1.574(2)	1.577
corrected for libration effects			
1	1.572	1.573	1.572
9	1.582	1.577	1.580

TABLE 2. Selected Bond Distances and Corrected Bond Distances for 18 and 19

compd	bond **a**	bond **b**	average (**a** and **b**)
18	1.548(2)	1.548(2)	1.548
19	1.554(2)	1.560(2)	1.557
corrected for libration effects			
18	1.551	1.553	1.552
19	1.556	1.561	1.559

substituted cycloadducts **9**−**11** and the furan cycloaducts **12**−**17**. Incorporation of an exo-trimethylsilyl substituent has been reported to increase the rate of the rDA by a factor of 95 (when X is $CH_2{=}CH_2$).[6] The origin of this rate enhancement was proposed to arise from charge stabilization of the polarized transition state from $\sigma_{C-Si}-\pi$ hyperconjugation involving the trimethylsilyl-group, which is antiperiplanar to the C−C bonds which break in this reaction.

Also of interest was to compare the structures of cycloadducts derived from furan, for which the barrier to the rDA reaction has been calculated to be ca. 37−40 kJ/mol lower than that for corresponding cyclopentadiene cycloadducts. This rate enhancement is believed to reflect the restoration of some aromatic character in the furan moiety at the transition state for the cycloreversion.[7] The facile rDA reaction of the furan−maleic anhydride cycloadduct is experimentally demonstrated by the rapid isomerization of the initially formed *endo* adduct **12** to the more stable *exo* adduct **15**. Furan cycloadducts are not only interesting due to their facile rDA reaction, but they also provide the opportunity to compare the structures of *endo* and *exo* cycloadducts, as these also have different reactivities; Lee *et al.* reported that the rate of the rDA reaction of the *endo* adduct **12** is 4 orders of magnitude greater than that of the *exo* adduct **15**.[8]

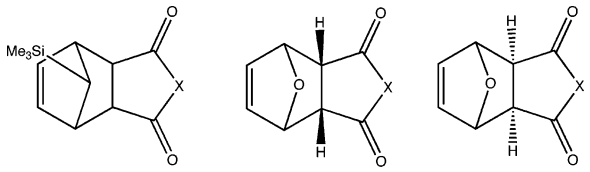

Results and Discussion

Trimethylsilyl-Substituted Cycloadducts. Trimethylsilyl-substituted cycloadducts **9**−**11** were prepared by combining 5-trimethylsilylcyclopentadiene[9] with maleic anhydride, *N*-methylmaleimide, and benzoquinone, respectively. Crystals suitable for X-ray analysis were obtained for adduct **9**; however, crystals of **10** and **11** were low quality and the resulting structural data, which had *R* factors of 6.5% and 12%, were deemed inaccurate for this study. Although this is a limited set of structural data, selected bond distances for **9** and the corresponding unsubstituted derivative **1**[2] for comparison are presented in Table 1, which also includes data corrected for thermal libration effects.[10]

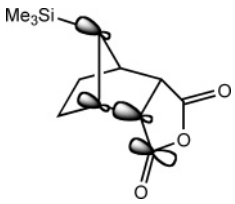

FIGURE 1. Through-bond orbital interactions in **19**.

TABLE 3. Selected Bond Distances for *Endo* and *Exo* Furan Adducts 13 and 16

compd	bond **a**	bond **b**	average (**a** and **b**)
13	1.571(2)	1.569(2)	1.570
16	1.563(2)	1.564(2)	1.564
corrected for libration effects			
13	1.578	1.573	1.576
16	1.567	1.566	1.567

TABLE 4. Selected Bond Distances for 1 and 2 and 13

compd	bond **a**	bond **b**	average (**a** and **b**)
1	1.569(2)	1.570(2)	1.570(2)
2	1.571(2)	1.570(2)	1.570(2)
13	1.571(2)	1.567(2)	1.569(2)
corrected for libration effects			
1	1.572	1.573	1.572
2	1.574	1.574	1.574
13	1.578	1.573	1.575

TABLE 5. Selected Bond Distances for 2, 15, 19, and 20

compd	bond **a**	bond **b**	average (**a** and **b**)	Δ (Å)
2	1.571(2)	1.570(2)	1.570	0.023
18	1.546(3)	1.548(3)	1.547	
15	1.564(2)	1.567(2)	1.566	0.042
20	1.524(2)	1.524(3)	1.524	
corrected for libration effects				
2	1.574	1.574	1.574	0.022
18	1.551	1.553	1.552	
15	1.573	1.570	1.572	0.044
20	1.527	1.527	1.527	

TABLE 6. Selected Bond Distances for Unsymmetrical Adducts 21−23

cycloadduct	C3−O3	C6−O3	bond **a**	bond **b**	Δ bond **a** and **b**
21	1.448(3)	1.434(3)	1.573(2)	1.565(2)	0.008
22	1.448(2)	1.437(2)	1.567(2)	1.569(2)	0.002
23			1.568(2)	1.548(2)	0.020
corrected for libration effects					
21	1.453	1.438	1.576	1.569	0.007
22	1.454	1.441	1.571	1.574	0.003
23			1.570	1.551	0.019

(6) Magnus, P.; Cairns, P. M.; Moursounidis, J. *J. Am. Chem. Soc*. **1987**, *109*, 2469

(7) Rulisek, L.; Sebek, P.; Havlas, Z.; Hrabal, R.; Capek, P. *J. Org. Chem.* **2005**, *70*, 6295.

(8) Lee, M. W.; Herdon, W. C. *J. Org. Chem*. **1978**, *43*, 518.

(9) Kralhanzel, C. S.; Losee, M. L. *J. Am. Chem. Soc*. **1969**, *90*, 4701.

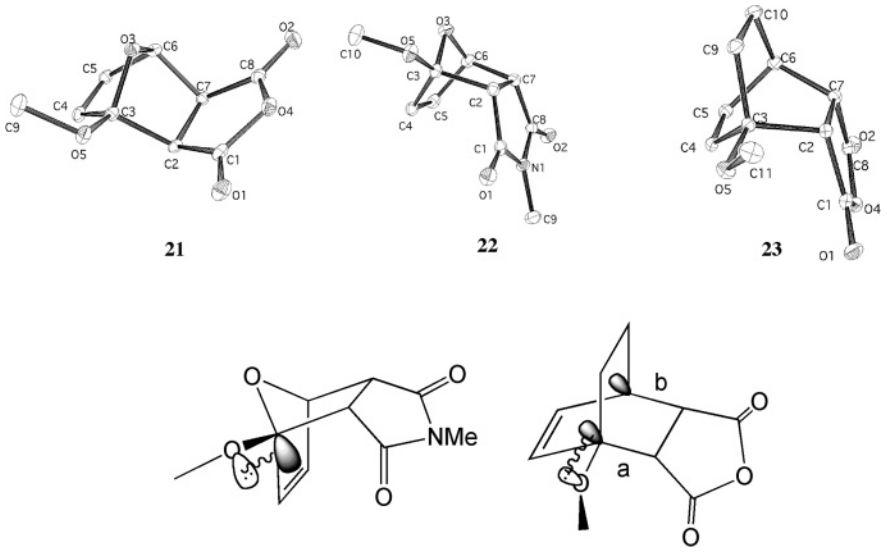

FIGURE 2. Ortep plots and orbital interaction diagrams for **21**−**23**; ellipsoids are at the 20% probability level.

These results show that, bonds **a** and **b** which break in the rDA reaction of **9** are on average 0.007 Å longer compared with those for **1** (0.008 Å when corrected for libration). Given the estimated standard deviation (esd) values of 0.002 Å on these distances, the lengthening of bonds **a** and **b** due to the presence of $SiMe_3$ is barely significant. Extra lengthening of bonds **a** and **b**, if taken as significant, might reflect the effects of $\sigma_{C-Si}-\sigma^*_{C-C}$ hyperconjugation between the antiperiplanar C−Si bond and bonds **a** and **b.** This is the same interaction that was proposed to stabilize the transition state for the rDA reaction of this substrate.[6] To gain further evidence for this interaction, the X-ray structures of the saturated analogues **18** and **19**, which were prepared from **2** and **9** by catalytic hydrogenation, were also determined. [Crystals of the saturated analogue of compound **1** did not provide data of satisfactory quality; previous work[2] suggests that comparison with the saturated analogue of **2** is justified.] Relevant structural parameters for **18** and **19** are summarized in Table 2.

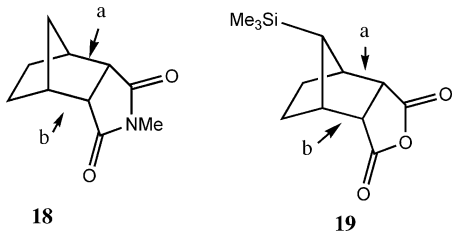

18 **19**

The saturated adduct **19** loses the effect of the $\pi-\sigma^*$ interaction, which causes lengthening of bonds **a** and **b**, and leads to the rDA reaction, but retains the $\sigma_{C-Si}-\sigma^*_{C-C}$ interaction. Interestingly the two C−C bonds (**a** and **b**), which are antiperiplanar to the $SiMe_3$ substituent, are 0.009 Å longer than the nonsubstituted adduct **18** (corrected is 0.007 Å). This bond lengthening can be described in orbital terms as an example of a Grob-like through-bond interaction between the σ_{C-Si} bonding orbital and the carbonyl π^* orbital, the geometrical requirements of which are well met within the bicyclic framework (Figure 1)

Furan Cycloadducts. The Diels−Alder reaction of furan with benzoquinone has been reported to occur at very high pressure;[11] however, our attempts to reproduce this result only returned starting materials. The Diels−Alder reaction between furan and maleic anhydride gave initially the *endo* cycloadduct **12** as judged by the ^{1}H NMR spectrum of the crude product; however, crystals of **12** for X-ray analysis could not be obtained, as isomerization to the more stable *exo* isomer **15** occurred during crystallization even at −20 °C. Suitable crystals for both the *endo* and *exo* isomers (**13** and **16**) of the slightly less reactive *N*-methylmaliemide cycloadduct were obtained by fractional crystallization of the crude reaction product. Selected structural data for **13** and **16** are summarized in Table 3.

The bonds **a** and **b** in the slightly more reactive *endo* isomer **13** are on average 0.006 Å longer compared to those of the more stable *exo* cycloadduct **16**, and this difference increases when libration corrections are applied (0.009 Å). This difference

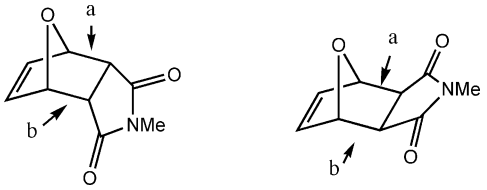

is comparable in magnitude to that calculated at the B3LYP-G31G* level for the *endo* and *exo* cycloadducts **12** and **15**.[12] The difference, which is very small, is only barely significant, but is consistent with the demonstrated higher reactivity of the *endo* isomer **13** compared to the *exo* isomer **16**.

Comparison of the structural parameters for these furan cycloadducts, with less reactive cyclopentadiene adducts, can be made by inspecting the structural parameters for **1**, **2**, and **13** all having the *endo* geometry; selected bond distances are summarized in Table 4.

Surprisingly the C−C bond distances in the *endo* furan cycloadduct **13** are not significantly different from those observed in the much less reactive cyclopentadiene cycloadducts

(10) Trueblood, K. N.; Maverick, E. F. *THMA11c*, A TLS Thermal Motion Analysis based on experimentally measured anisotropic displacement parameters available from the following WEB site: www.chem.gla.ac.uk/~louis/thma14/.

(11) Jurczak, J.; Kozluk, T.; Filipek, S.; Euster, C. H. *Helv. Chim. Acta* **1983**, *66*, 222.

(12) Calvo-Losada, S.; Suarez, D. *J. Am. Chem. Soc.* **2000**, *122*, 390.

SCHEME 1

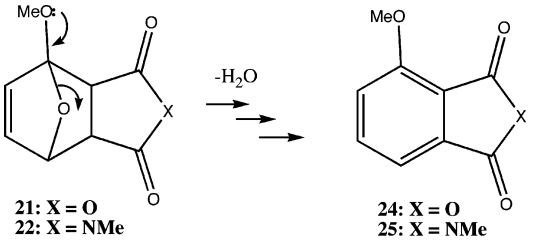

21: X = O
22: X = NMe

24: X = O
25: X = NMe

1 and **2**. This appeared to be counter to the predictions of the structure correlation principle. A possible explanation is that the presence of the electronegative oxygen of the furan moiety decreases the "natural" C−C bond distances (**a** and **b**) to the bridgehead carbons, suggesting that perhaps a direct comparison between these bond distances with the corresponding distances in the cyclopentadiene cycloadducts is not justified. Thus it was deemed more appropriate to determine the degree of lengthening of the C−C bond distances in the furan cycloadducts compared with their corresponding saturated analogues, which cannot undergo the rDA reaction, and compare this to the degree of lengthening of the C−C bonds in the cyclopentadiene cycloadducts with their saturated analogues. After reduction of the furan cycloadducts **12**−**17** by hydrogenation the only suitable crystals for X-ray analysis were obtained for the saturated *exo* furan maleic anhydride cycloadduct **20**, which was compared with the exo cycloadduct **15**. Selected data for compounds **2**, **18**, **15**, and **20** are presented in Table 5.

From these data it is quite clear that the "natural" C−C bond distances to the bridgehead carbons as provided by the saturated furan cycloadduct **20** are significantly shorter than the similar

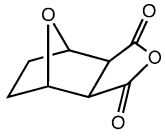

20

C−C bonds in the saturated cyclopentadiene adduct **18**, thus demonstrating that the electronegative oxygen does indeed exert a marked "bond-shortening" effect. This effect can be more generally demonstrated from a search of the Cambridge Crystallographic database.[13] Molecules containing the C−C−O fragment gave a mean C−C distance of 1.531 Å while similar C−C−C fragments had a mean C−C distance of 1.547 Å. Importantly, these data show that the degree of bond lengthening observed in the furan cycloadduct **15** relative to the saturated analogue **20**, which is 0.042 Å, is significantly greater than the degree of bond lengthening observed in the cyclopentadiene cycloadduct **2**, which is 0.023 Å. Thus, according to the structure correlation principle,[5] this is consistent with the greater reactivity of the furan cycloadducts toward the rDA reaction.

The structural effects arising in the cycloadducts of 2-methoxyfuran with maleic anhydride and *N*-methylmaleimide were investigated, as previous reports suggest that cycloadditions involving 2-methoxyfuran as dienophile proceed in a stepwise fashion.[14] We therefore expected there to be marked differences in the lengths of bonds **a** and **b** in the ground state in accord with previous observations on the cyclohexadiene cycloadduct **8**.[4] Thus the *exo* cycloadducts **21** and *endo* cycloadduct **22** were prepared by combining 2-methoxyfuran with maleic anhydride and *N*-methylmaleimide, respectively. Crystals of suitable quality for X-ray analysis were obtained at −20 °C. Selected structural data for **21** and **22** are presented in Table 6, in addition to the previously determined cycloadduct **23**,[4] which is included here for comparison.

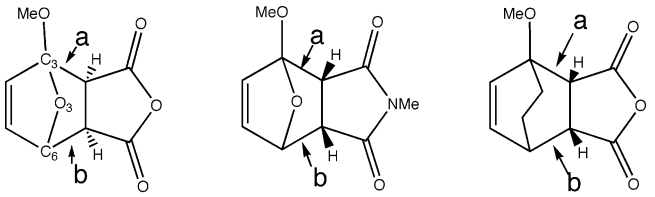

21 **22** **23**

Surprisingly, there was found to be very little difference in the bond distances **a** and **b** in both **21** and **22**, which contrasts with the result obtained for **23** where the difference is much more significant. An explanation for this "anomalous" result is provided by examination of the conformation of the OCH_3 substituent as defined by the CH_3−O−C3−C2 dihedral angle. In compound **23** the CH_3−O−C3−C2 dihedral angle is 69.1-(2)°, which allows for effective overlap of a nonbonded orbital on the oxygen with the C3−C2 σ^* orbital (Figure 2); it is this interaction that was proposed to cause the extra lengthening of bond **a** compared to bond **b**.[4] However, in compounds **21** and **22** the CH_3−O−C3−C2 dihedral angles are 177.9° and 180.0°, respectively, which places the OCH_3 group antiperiplanar to the C3−C2 bond, resulting in overlap of a nonbonded orbital on the oxygen with the bridging C−O σ^* orbital (Figure 2) rather than with the C3−C2 σ^* orbital. Consistent with this is significant asymmetry in the two C−O bond distances involving the bridging oxygen (Table 6). The C3−O3 distance is significantly longer than the C6−O3 distance, which is an example of the structural anomeric effect that has been described previously for other oxygen-containing systems.[15]

Interesting, upon standing at room temperature, cycloaducts **21** and **22** both underwent decomposition giving the aromatic products **24** and **25**, respectively, by initial cleavage of the C3−O bond followed by aromatization by elimination of H_2O. The initial step of this rearrangement no doubt involves the same interaction causing lengthening of the C3−O bond distance (Scheme 1).

Conclusions

Relationships between structure and reactivity are demonstrated by comparing the trimethysilylcyclopentadiene−maleic anhydride cycloadduct **9** with the silicon-free analogue **1**, and by comparison of the *endo* and *exo* isomers of furan cycloadducts **13** and **16**. The C−C bonds, which break in the retro-Diels−Alder (rDA) reaction for these structures, are slightly longer in the more reactive derivatives. This effect is small, thus demonstrating that small increases in C−C bond distance have a large effect on the rDA reactivity. However, care must be taken when comparing C−C bond distances in unlike systems, for example, the bond distances for the C−C bonds

(13) Allen, F. H.; Bellard, S.; Brice, M. D.; Cartwright, B. A.; Doubleday, A.; Higgs, H.; Hummelink, T.; Hummelink-Peters, T.; Kennard, O.; Motherwell, W. D. S.; Rogers, J. R.; Watson, D. G. *Acta Crystallogr*. **1979**, *B35*, 2331.

(14) Bridson, J. N.; Bennett, S. M.; Butler, G. *J. Chem. Soc., Chem. Commun.* **1980**, 413.

(15) Kirby, A. J. *The Anomeric Effect and Related Stereoelectronic Effects at Oxygen*; Springer-Verlag: New York, 1983.

TABLE 7. Crystal Data and Structure Refinement Details for Compounds 9−11, 13, 15, 16, 19, 20, 21, and 22

	9	**10**	**11**	**13**	**15**
empirical formula	$C_{12}H_{16}O_3Si$	$C_{13}H_{19}NO_2Si$	$C_{13}H_{17}O_2Si$	$C_9H_9NO_3$	$C_8H_6O_4$
formula weight	236.34	249.38	233.36	179.17	177.13
temperature (°C)	130(2)	130(2)	130.0(1)	130(2)	130(2)
radiation	MoKα	MoKα	MoKα	MoKα	MoKα
wavelength (Å)	0.71073	0.71073	0.71073	0.71073	0.71073
crystal system	monoclinic	monoclinic	triclinic	monoclinic	orthorhombic
space group	$P2_1/c$	$P2_1/c$	$P\bar{1}$	$P2_1/c$	$P2_12_12_1$
unit cell dimensions					
a (Å)	12.636(2)	21.4178(17)	6.556(1)	12.1591(13)	5.3600(12)
b (Å)	6.498(1)	29.654(2)	10.968(2)	10.3998(11)	6.9759(15)
c (Å)	15.649(3)	6.4401(5)	19.259(3)	6.8354(8)	18.844(4)
α (deg)	90	90	75.350(3)	90	90
β (deg)	107.573(3)	91.594(2)	87.190(4)	104.382(2)	90
γ (deg)	90	90	89.440(3)	90	90
volume (Å^3)	1225.0(4)	4088.7(6)	1338.1(4)	838.3(2)	704.6(3)
Z	4	12	4	4	4
D_c (Mg/m^3)	1.281	1.215	1.158	1.421	1.566
μ (mm^{-1})	0.181	0.163	0.091	0.108	0.128
F(000)	504	1608	500	376	344
crystal size	0.20 × 0.20 × 0.15	0.5 × 0.25 × 0.1	0.25 × 0.15 × 0.05	0.30 × 0.10 × 0.05	0.50 × 0.15 × 0.05
θ range (deg)	1.69 to 27.51	0.95 to 25.00	1.09 to 27.55	1.73 to 25.00	2.16 to 27.51
no. of refx collected	7436	21654	8392	5889	4400
independent	2792	7197	5852	1473	1592
R(int)	0.0340	0.068	0.0602	0.0856	0.0656
observed ($I > 2\sigma(I)$)	2193	5425	3770	1397	1450
data/restraints/param	2792/0/149	7197/0/470	5852/0/315	1473/0/120	1592/0/110
GOF on F^2	0.980	1.092	1.059	1.058	1.020
final *R* indices	0.0415	0.0656	0.1233	0.0481	0.0407
[$I > 2\sigma(I)$]	$wR2 = 0.1003$	$wR2 = 0.1415$	$wR2 = 0.3194$	$wR2 = 0.1210$	$wR2 = 0.0977$
R indices	0.0522	0.0887	0.1690	0.0498	0.0440
(all data)	$wR2 = 0.1052$	$wR2 = 0.1521$	$wR2 = 0.3580$	$wR2 = 0.1226$	$wR2 = 0.0998$
weighting scheme:[a] *A*	0.0577	0.059	0.1896	0.0507	0.0535
weighting scheme:[a] *B*	0	0.30	2.38	0.35	0
largest diff peak/hole (eÅ^{-3})	0.313/−0.265	0.394/−0.340	3.5/−0.4	0.202/−0.195	0.235/−0.190

	16	**19**	**20**	**21**	**22**
empirical formula	$C_9H_9NO_3$	$C_{12}H_{18}O_3Si$	$C_8H_8O_4$	$C_9H_8O_5$	$C_9H_9NO_3{\cdot}[C_2H_5OH{\cdot}H_2O]$
formula weight	179.17	238.35	168.14	195.15	273.28
temperature (°C)	130(2)	130(2)	130(2)	130.0(1)	130(2)
radiation	MoKα	Mo Kα	Mo Kα	Mo Kα	Mo Kα
wavelength (Å)	0.71073	0.71073	0.71073	0.71073	0.71073
crystal system	monoclinic	monoclinic	orthorhombic	monoclinic	monoclinic
space group	$P2_1/c$	$P2_1/c$	$Pna2_1$	$C2/c$	$P2_1/n$
unit cell dimensions					
a (Å)	6.6227(3)	12.930(2)	10.448(3)	25.166(6)	8.8817(8)
b (Å)	15.9098(8)	6.3374(8)	6.5388(15)	5.3338(13)	8.1183(7)
c (Å)	7.7878(4)	15.771(2)	10.263(2)	13.990(4)	17.240(2)
α (deg)	90	90	90	90	90
β (deg)	98.204(1)	107.937(2)	90	117.184(4)	98.569(2)
γ (deg)	90	90	90	90	90
volume (Å^3)	812.17(7)	1229.5(4)	701.1(3)	1670.4(7)	1229.2(2)
Z	4	4	4	8	4
D_c (Mg/m^3)	1.465	1.288	1.593	1.560	1.421
μ (mm^{-1})	0.111	0.181	0.129	0.130	0.108
F(000)	376	512	352	816	584
crystal size	0.45 × 0.30 × 0.15	0.40 × 0.30 × 0.2	0.5 × 0.2 × 0.1	0.5 × 0.15 × 0.1	
θ range (deg)	2.56 to 27.50	1.66 to 25.00	3.68 to 24.99	1.82 to 24.98	2.39 to 25.00
no. of refx collected	6944	5470	3366	4185	6234
independent	1859	2157	1205	1476	2158
R(int)	0.0392	0.0546	0.049	0.1003	0.0416
observed ($I > 2\sigma(I)$)	1743	1721	1154	1032	1886
data/restraints/param	1859/0/119	2157/0/148	1205/0/109	1476/0/129	2158/0/137
GOF on F^2	1.052	0.972	1.032	0.907	1.042
final *R* indices	0.0493	0.0395	0.0414	0.0467	0.0470
[$I > 2\sigma(I)$]	$wR2 = 0.1355$	$wR2 = 0.0933$	$wR2 = 0.0970$	$wR2 = 1006$	$wR2 = 0.1195$
no. of *R* indices	0.0512	0.0506	0.0431	0.0695	0.0524
(all data)	$wR2 = 0.1371$	$wR2 = 0.972$	$wR2 = 0.0979$	$wR2 = 0.1072$	$wR2 = 0.1228$
weighting scheme:[a] *A*	0.0741	0.0478	0.0668	0.0432	0.0484
weighting scheme:[a] *B*	0.494	0	0	0	0.81
largest diff peak/hole (eÅ^{-3})	0.58/−0.26	0.309/−0.213	0.214/−0.178	0.223/−0.222	0.266/−0.186

[a] $w = 1/[\sigma^2(F_o^2) + (A*P)^2 + B*P]$, where $P = (F_o^2 + 2F_c^2)/3$.

that break in the rDA for cyclopentadiene cycloadducts cannot be directly compared with the more reactive furan cycloadducts. It is thus more appropriate in these cases to compare the degree of bond lengthening with respect to an appropriate model system that cannot undergo the rDA reaction.

The structures of the 2-methoxyfuran cycloadducts **22** and **23** provided an insight into the observed instability of these compounds in solution.

Experimental Section

(1) X-ray Crystallography. Intensity data were collected with a Bruker SMART Apex CCD detector, using Mo Kα radiation (graphite crystal monochromator $\lambda = 0.71073$). Data were reduced with use of the program SAINT. The temperature during data collection was maintained at 130.0(1) with an Oxford Cryostream cooling device. The structures were solved by direct methods and difference Fourier synthesis. Thermal ellipsoid plots were generated with the program ORTEP-3[16] integrated within the WINGX[17] suite of programs. Crystal data and structure refinement details are summarized in Table 7. Corrections for the effects of thermal libration were carried out with the Thma11 program.[10]

(2) Synthesis. General experimental details are reported elsewhere.[3] 5-Trimethylsilylcyclopentadiene was prepared according to the literature procedure.[9] Accurate mass data were collected on a Waters LCT Premier XE time-of-flight mass spectrometer.

Cycloadduct 9. Maleic anhydride (0.551 g, 5.62 mmol) in diethyl ether (10 mL) and 5-trimethylsilylcyclopentadiene (0.802 g, 5.81 mmol) in diethyl ether (15 mL) were stirred at room temperature under nitrogen for 6 h. The solvent was removed under reduced pressure and the crude product was recrystallized from pentane to give cycloadduct **9** as colorless crystals (0.916 g, 3.88 mmol, 69%), mp 99−100 °C (lit.[5] mp 98−99 °C). ^{1}H NMR ($CDCl_3$) δ 6.24 (2H, t, $J = 1.7$ Hz), 3.62 (2H, dd, $J = 1.7$ Hz, 1.5 Hz) 3.55 (2H, t, $J = 15$ Hz), 1.26 (1H, s), −0.042 (9H, s); ^{13}C NMR ($CDCl_3$) δ 171.0, 135.0, 56.9, 49.4, 49.1, −0.5.

Cycloadduct 10. *N*-Methylmaleimide (0.201 g, 1.81 mmol) and 5-trimethylsilylcyclopentadiene (0.278 g, 2.01 mmol) in diethyl ether (15 mL) were stirred at room temperature for 8 h. The crude product was recrystallized from hexane to give colorless crystals (0.393 g, 1.58 mmol, 87%), mp 91−93 °C. ^{1}H NMR ($CDCl_3$) δ 6.00 (2H, t, $J = 2.0$ Hz), 3.41 (2H, br s), 3.55 (2H, br s), 2.79 (3H, s), 1.22 (1H, s), −0.07 (9H, s); ^{13}C NMR ($CDCl_3$) δ 177.7, 133.9, 55.9, 48.4, 47.6, 24.1, −0.4. MH+ 250.1264 calcd for $C_{13}H_{19}NO_2Si$ 250.1263.

Cycloadduct 11.[18]Benzoquinone (0.199 g, 1.84 mmol) and 5-trimethylsilylcyclopentadiene (0.254 g, 1.84 mmol) in diethyl ether (15 mL) were stirred at room temperature for 4 h. The crude product was recrystallized from hexane to give **11** as yellow crystals (0.397 g, 1.62 mmol, 88%), mp 86−87 °C. ^{1}H NMR ($CDCl_3$) δ 6.53 (2H, t, $J = 2.2$ Hz), 5.97 (2H, d, $J = 1.9$ Hz), 3.61 (2H, br s), 3.22 (2H, d, $J = 1.5$ Hz), 1.06 (1H, s), −0.07 (9H, s); ^{13}C NMR ($CDCl_3$) δ 178.0, 139.0, 135.4, 57.0, 49.9, 49.2, −0.5.

Preparation of Compound 19. A mixture of cycloadduct **9** (0.500 g, 2.12 mmol) and 5% palladium on carbon (120 mg) in tetrahydrofuran (50 mL) was stirred under hydrogen at room temperature and atmospheric pressure. After consumption of 1 molar equiv of hydrogen (50 mL), the reaction mixture was filtered through celite and the solvent was removed under reduced pressure. The crude product was recrystallized from pentane to give **19** as colorless crystals (0.46 g, 1.93 mmol, 91%), mp 107−109 °C. ^{1}H NMR ($CDCl_3$) δ 3.41 (2H, br s), 2.91 (2H, br s) 1.69 (2H, m), 1.45 (2H, m), 1.08 (1H, s), 0.05 (9H, s); ^{13}C NMR ($CDCl_3$) δ 171.9, 54.4, 45.6, 43.0, 24.9, −1.0. MH+ 239.10978 calcd for $C_{12}H_{19}O_3Si$ 239.10980.

Cycloadduct 15. Maleic anhydride (0.648 g, 6.61 mmol) and furan (0.500 g, 7.34 mmol) in tetrahydrofuran (10 mL) were stirred together at room temperature for 16 h. The crude product was recrystallized from ethyl acetate to give **15** as colorless crystals (0.713 g, 4.30 mmol, 65%), mp 114−115 °C (lit.[8] mp 110 °C). ^{1}H NMR ($CDCl_3$) δ 6.59 (2H, d, $J = 3.2$ Hz), 5.46 (2H, d, $J = 3.2$ Hz), 3.20 (2H, m); ^{13}C NMR ($CDCl_3$) δ 168.3, 137.0, 82.2, 48.7.

Cycloadducts 13 and 16. *N*-Methylmaleimide (0.816 g, 7.34 mmol) and furan (1.000 g, 14.6 mmol) in tetrahydrofuran (10 mL) were reacted at room temperature for 48 h. The crude product was fractionally crystallized from ethyl acetate to give colorless crystals (0.802 g, 4.48 mmol, 61%), mp 138−140 °C (lit.[8] mp 138−141 °C). *Endo* isomer **13**: ^{1}H NMR ($CDCl_3$) δ 6.40 (2H, s), 5.33 (2H, d, $J = 4.2$ Hz), 3.53 (2H, d, $J = 4.2$ Hz), 2.82 (3H, s); ^{13}C NMR ($CDCl_3$) δ 175.1, 134.3, 79.4, 46.2, 24.6. *Exo* isomer **16**: ^{1}H NMR ($CDCl_3$) δ 6.50 (2H, s), 5.30 (2H, d, $J = 4.0$ Hz), 3.53 (2H, d, $J = 4.0$ Hz), 3.13 (3H, s); ^{13}C NMR ($CDCl_3$) δ 174.2, 131.3, 79.3, 47.2, 24.5.

Cycloadduct 21 and Rearrangement Product 24. Maleic anhydride (0.450 g, 4.59 mmol) and 2-methoxyfuran (0.500 g, 5.10 mmol) in diethyl ether (10 mL) were stirred at room temperature for 48 h. Removal of the solvent and recrystallized of the crude product from ethyl acetate gave cycloadduct **21** as colorless crystals (0.774 g, 3.95 mmol, 86%), mp 121−124 °C (lit.[9] mp 120−121 °C). ^{1}H NMR ($CDCl_3$) δ 6.72 (1H, dd, $J = 2$ Hz, 5.7 Hz), 6.54 (1H, d, $J = 5.7$ Hz), 5.27 (1H, d, $J = 2$ Hz), 3.64 (3H, s), 3.37 (1H, d, $J = 6.5$ Hz), 3.24 (1H, d, $J = 6.5$ Hz); ^{13}C NMR ($CDCl_3$) δ 169.9, 166.3, 139.8, 135.7, 103.9, 76.7, 55.6, 53.0, 49.0.

Upon standing at room temperature cycloadduct **21** turned to a yellow oil. The ^{1}H NMR of the yellow oil was consistent with the literature data reported for compound **24**.[19] ^{1}H NMR ($CDCl_3$) δ 7.82 (1H, t, $J = 8.1$ Hz), 7.57 (1H, d, $J = 8.0$ Hz), 7.33 (1H, d, $J = 8.0$ Hz), 4.08 (3H, s).

Cycloadduct 22. *N*-Methylmaleimide (0.500 g, 4.50 mmol) and 2-methoxyfuran (0.486 g, 4.95 mmol) in diethyl ether (10 mL) were stirred at room temperature for 30 h. The crude product was recrystallized from hexane to give cycloadduct **22** as colorless crystals (0.469 g, 2.24 mmol, 50%), mp 135−136 °C. ^{1}H NMR ($CDCl_3$) δ 6.48 (1H, dd, $J = 1.7$ Hz, 5.9 Hz), 6.41 (1H, d, $J = 5.9$ Hz), 5.14 (1H, m), 3.74 (1H, m), 3.59(3H, s), 3.36 (1H, d, $J = 7.6$ Hz), 2.84 (3H, s); ^{13}C NMR ($CDCl_3$) δ 174.2, 173.7, 136.4, 133.1, 114.4, 73.7, 54.1, 48.7, 47.8, 24.1. MH+ 210.07607 calcd for $C_{10}H_{12}NO_4$ 210.07608.

Acknowledgment. Our gratitude goes to the University of Melbourne for MIRS and MIFRS scholarships, and an Albert Shimmins Fund award to Goh Yit Wooi. Thanks also go to Dr. Simon Egan and Asimo Karnezis for kindly acquiring HRMS at short notice.

Supporting Information Available: NMR spectra (^{1}H and ^{13}C) for compounds **10** and **19** and libration corrections for compounds **9**, **10**, **13**, **15**, **16**, **19**, **20**, **21**, and **22**. This material is available free of charge via the Internet at http://pubs.acs.org.

JO7018575

(16) Farrugia, L. J. *J. Appl. Crystallogr.* **1997**, *30*, 565.
(17) Farrugia, L. J. *J. Appl. Crystallogr.* **1999**, *32*, 837.
(18) Tolstikov, G. A.; Lerman, B. M.; Galin, F. Z.; Danilova, N. A. *Zh. Obsh. Khim.* **1977**, *47*, 1656.
(19) Gupta, D. N.; Hodge, P.; Hurley, P. N. *J. Chem. Soc., Perkin Trans. 1* **1989**, 391.